Online appendix for "A penalized distributed lag non-linear Lee-Carter framework for regional weekly mortality forecasting"

Jens Robben[1,*] and Karim Barigou[2]

[1] *Research Centre for Longevity Risk (RCLR), Faculty of Economics and Business, University of Amsterdam, Amsterdam, the Netherlands.*
[2] *Institute of Statistics, Biostatistics and Actuarial Science (ISBA), Louvain Institute of Data Analysis and Modeling (LIDAM), UCLouvain, Louvain-la-Neuve, Belgium*

A Supplementary figures

In-sample fit of death rates. Figures 1, 2, 3, 4, 5, 6, 7, 8, 9, and 10 show the estimated death rates on a logarithmic scale in the twelve administrative regions in France for the age groups 50-54, 55-59, 60-64, 65-69, 70-74, 75-79, 80-84, 85-89, 90-94, and 95+, respectively. We show the fit as obtained by the baseline model and the full model including the DLNMs for temperature and influenza.

Pearson residuals. Figure 11 visualizes the squared Pearson residuals across age and time for the twelve administrative regions in France.

Uncertainty bounds. Figure 12 visualizes the 95% uncertainty bounds around the logarithm of the estimated weekly death rates from 1990-2019 for the age groups 50-54, 70-74 and 90-94 in the twelve administrative regions of France.

Overall relative risk. Figures 13 and 14 show the estimated overall relative risk for temperature and ILI exceedance rates in the twelve administrative regions of France for the age groups 50–54, 70–74, and 90–94.

Relative risk by lag. Figures 15 and 16 present the estimated lag-specific relative risks at the 99.5th percentile of the region-specific weekly average temperatures and ILI exceedance rates, respectively, for the twelve administrative regions of France and for the age groups 50-54, 70-74, and 90-94.

Relative risk surface. Figures 17 and 18 visualize the estimated relative risk (RR) surfaces of the lag-specific temperature and ILI mortality associations in the 12 administrative regions of France for the age group 90–94.

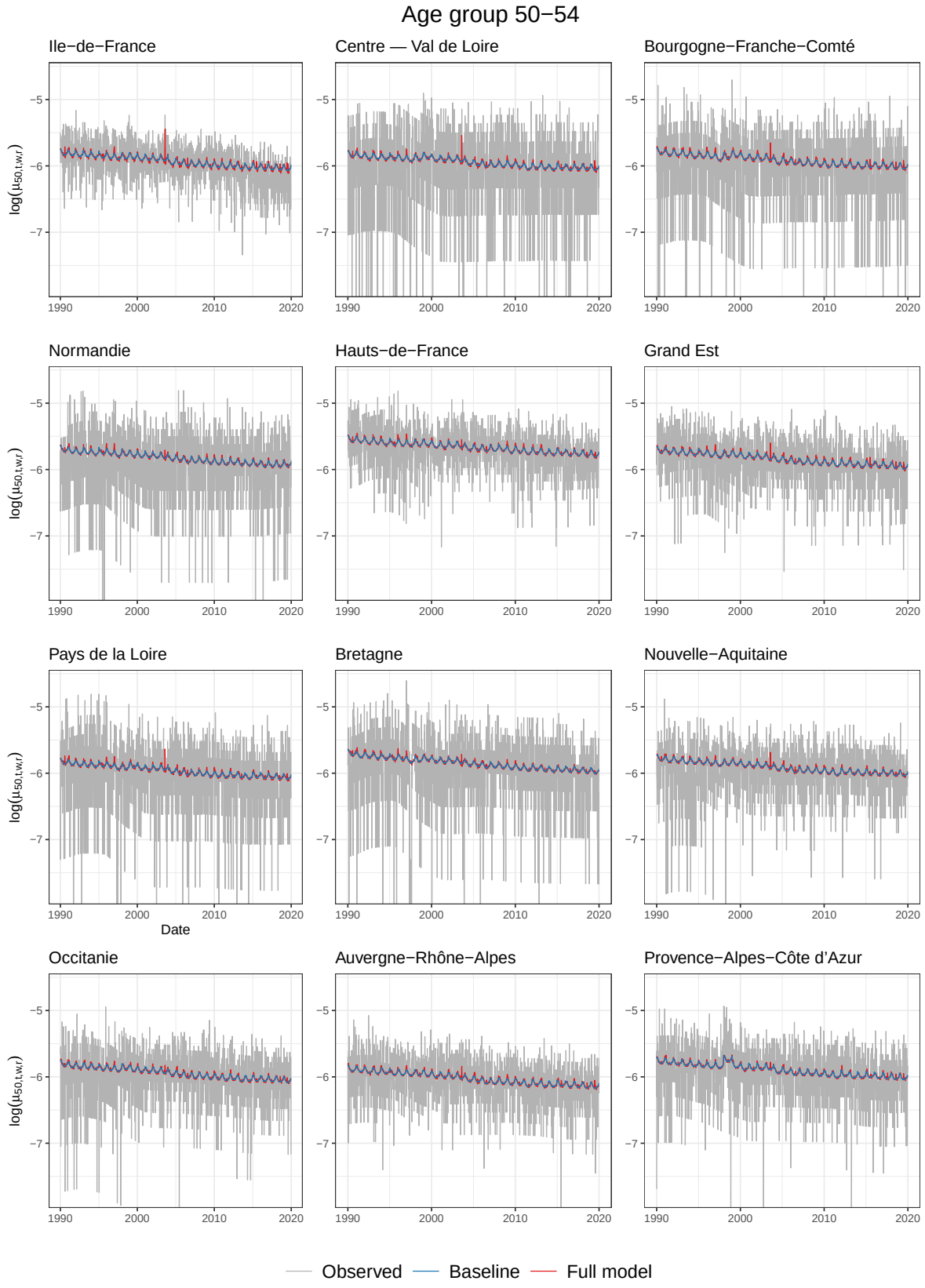

Figure 1: Estimated female weekly death rates from 1990-2019 for the age group 50–54. The gray line represents the logarithm of the observed death rates, while the blue and red line reflect the logarithm of the death rates estimated by the baseline and the full model, including the DLNM component, respectively.

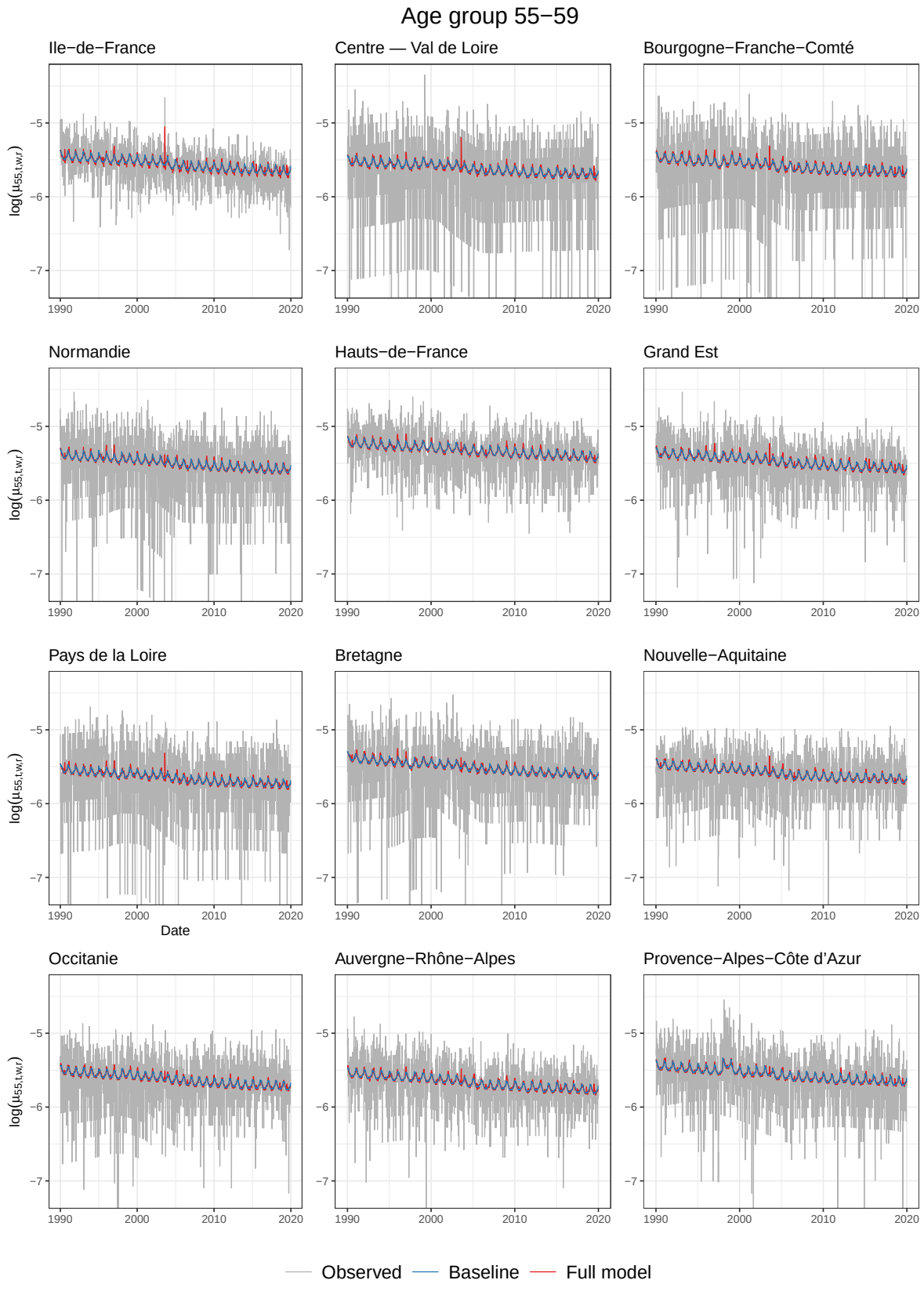

Figure 2: Estimated female weekly death rates from 1990-2019 for the age group 55–59. The gray line represents the logarithm of the observed death rates, while the blue and red line reflect the logarithm of the death rates estimated by the baseline and the full model, including the DLNM component, respectively.

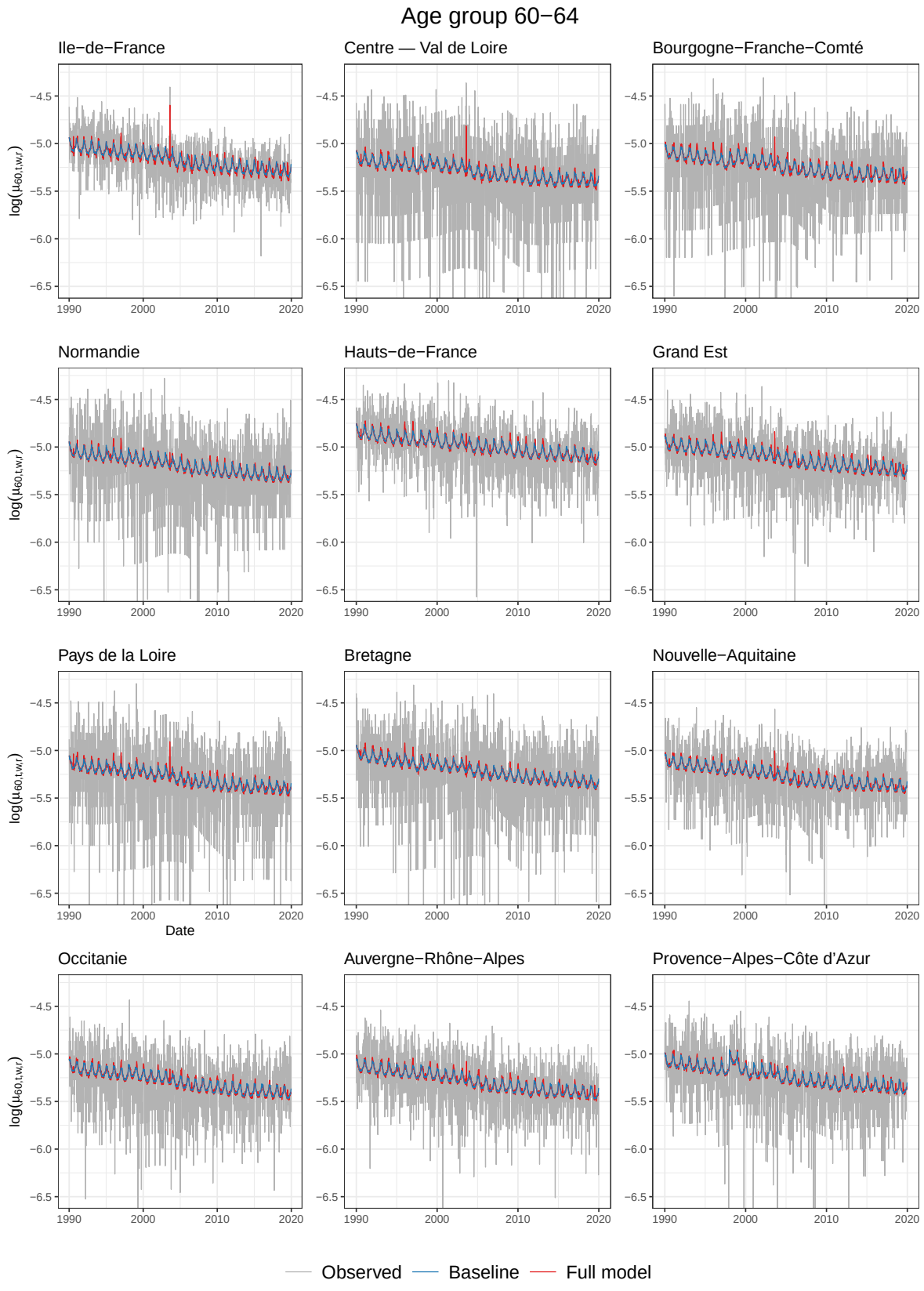

Figure 3: Estimated female weekly death rates from 1990-2019 for the age group 60–64. The gray line represents the logarithm of the observed death rates, while the blue and red line reflect the logarithm of the death rates estimated by the baseline and the full model, including the DLNM component, respectively.

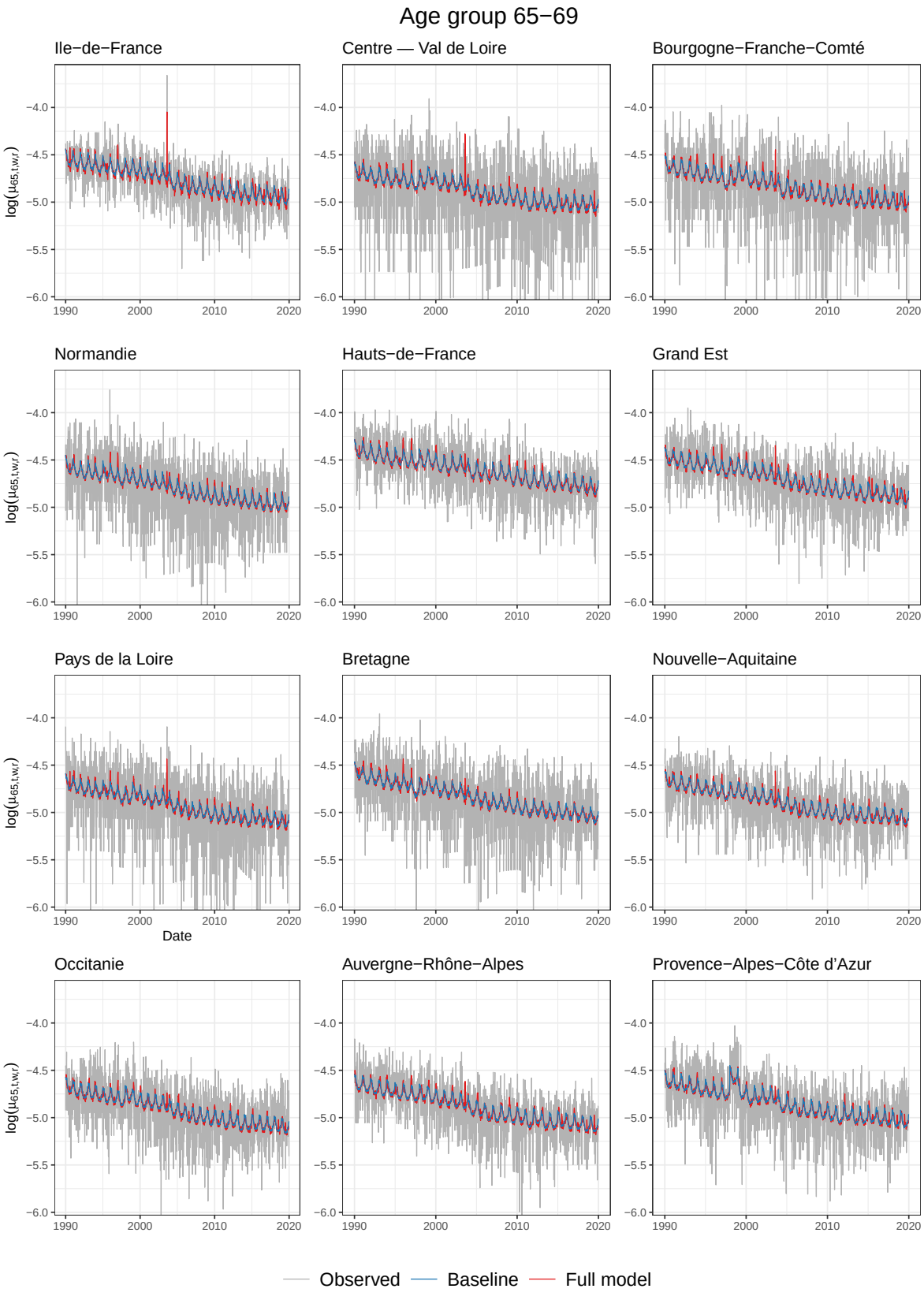

Figure 4: Estimated female weekly death rates from 1990-2019 for the age group 65–69. The gray line represents the logarithm of the observed death rates, while the blue and red line reflect the logarithm of the death rates estimated by the baseline and the full model, including the DLNM component, respectively.

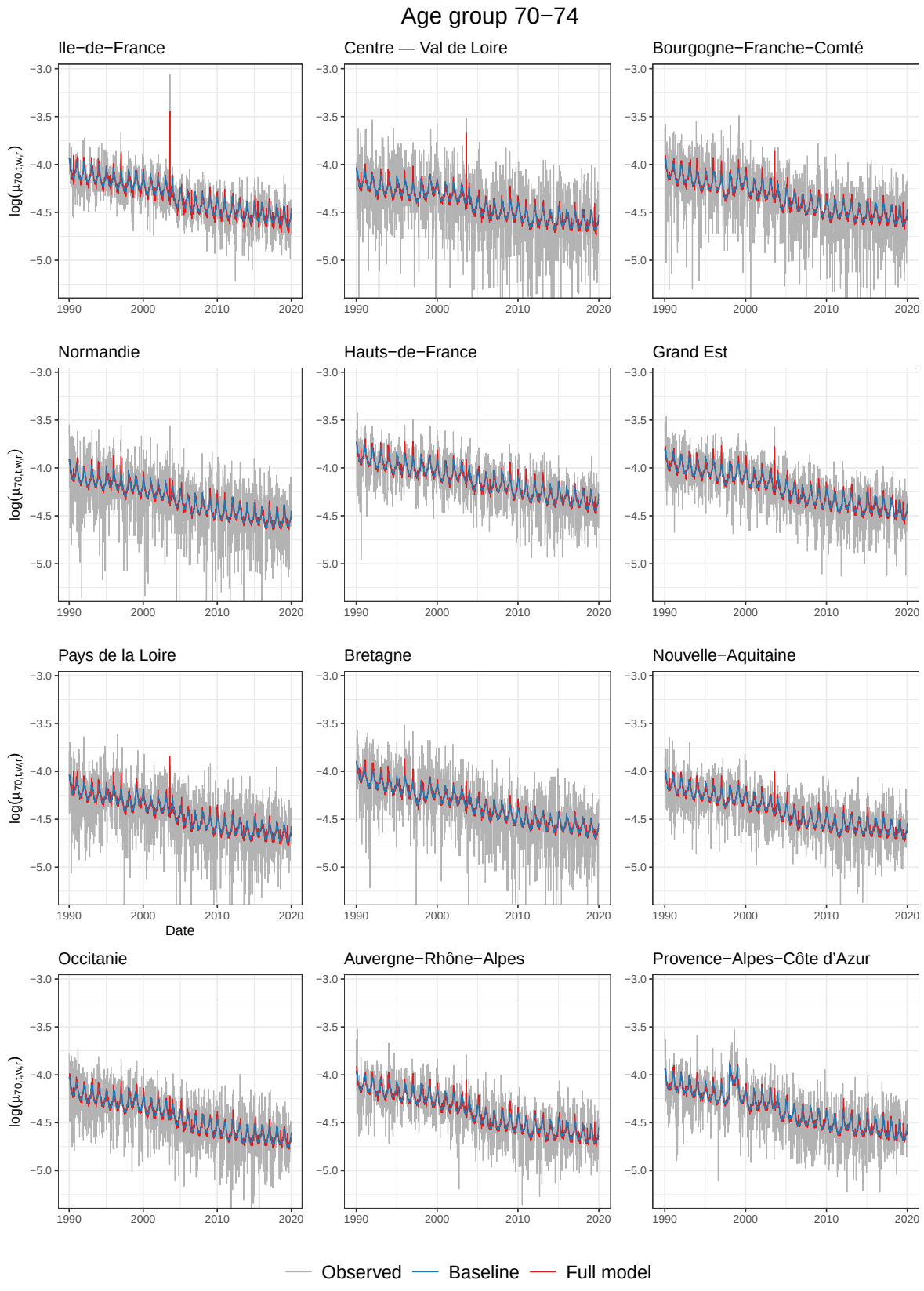

Figure 5: Estimated female weekly death rates from 1990-2019 for the age group 70–74. The gray line represents the logarithm of the observed death rates, while the blue and red line reflect the logarithm of the death rates estimated by the baseline and the full model, including the DLNM component, respectively.

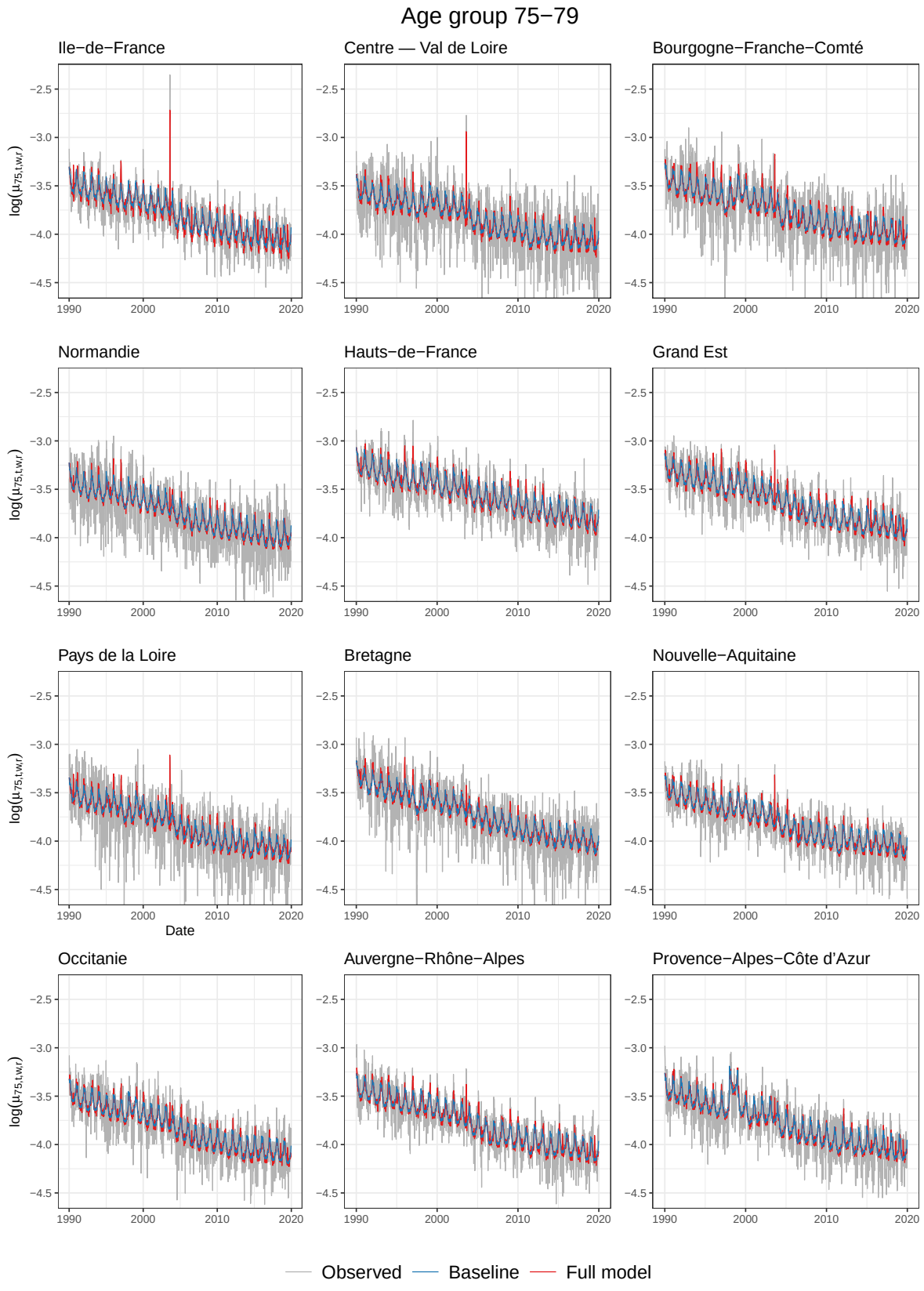

Figure 6: Estimated female weekly death rates from 1990-2019 for the age group 75–79. The gray line represents the logarithm of the observed death rates, while the blue and red line reflect the logarithm of the death rates estimated by the baseline and the full model, including the DLNM component, respectively.

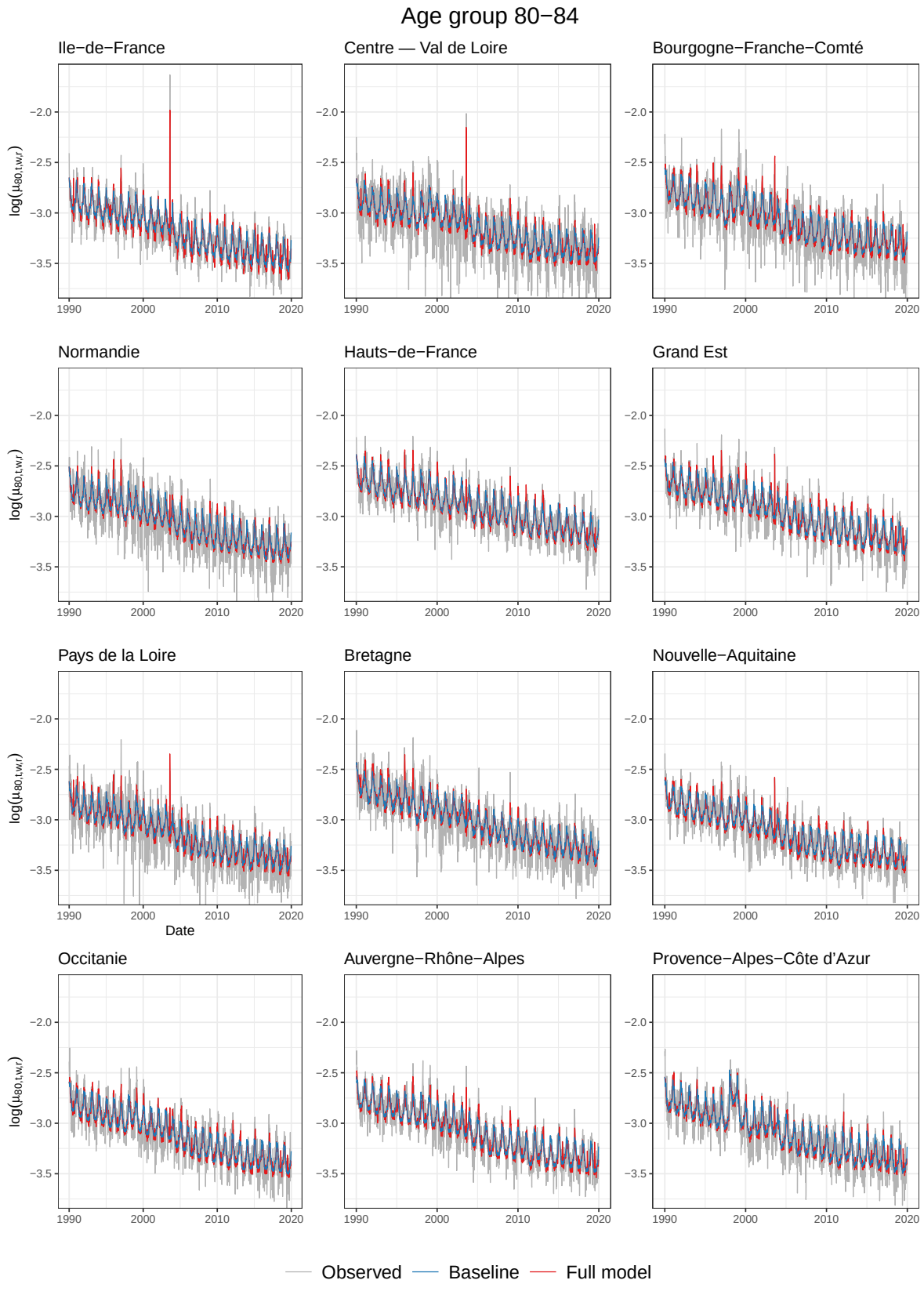

Figure 7: Estimated female weekly death rates from 1990-2019 for the age group 80–84. The gray line represents the logarithm of the observed death rates, while the blue and red line reflect the logarithm of the death rates estimated by the baseline and the full model, including the DLNM component, respectively.

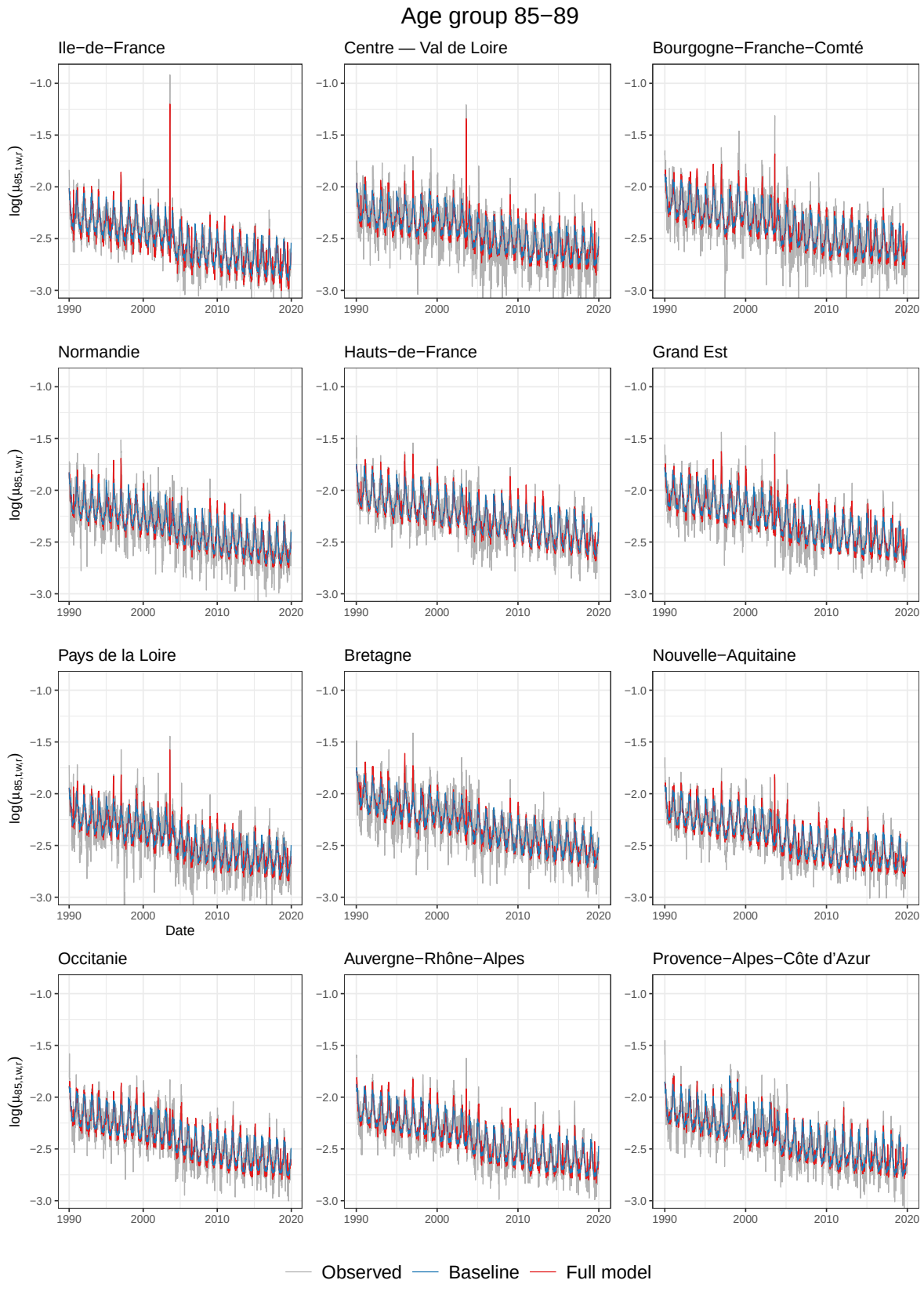

Figure 8: Estimated female weekly death rates from 1990-2019 for the age group 85–89. The gray line represents the logarithm of the observed death rates, while the blue and red line reflect the logarithm of the death rates estimated by the baseline and the full model, including the DLNM component, respectively.

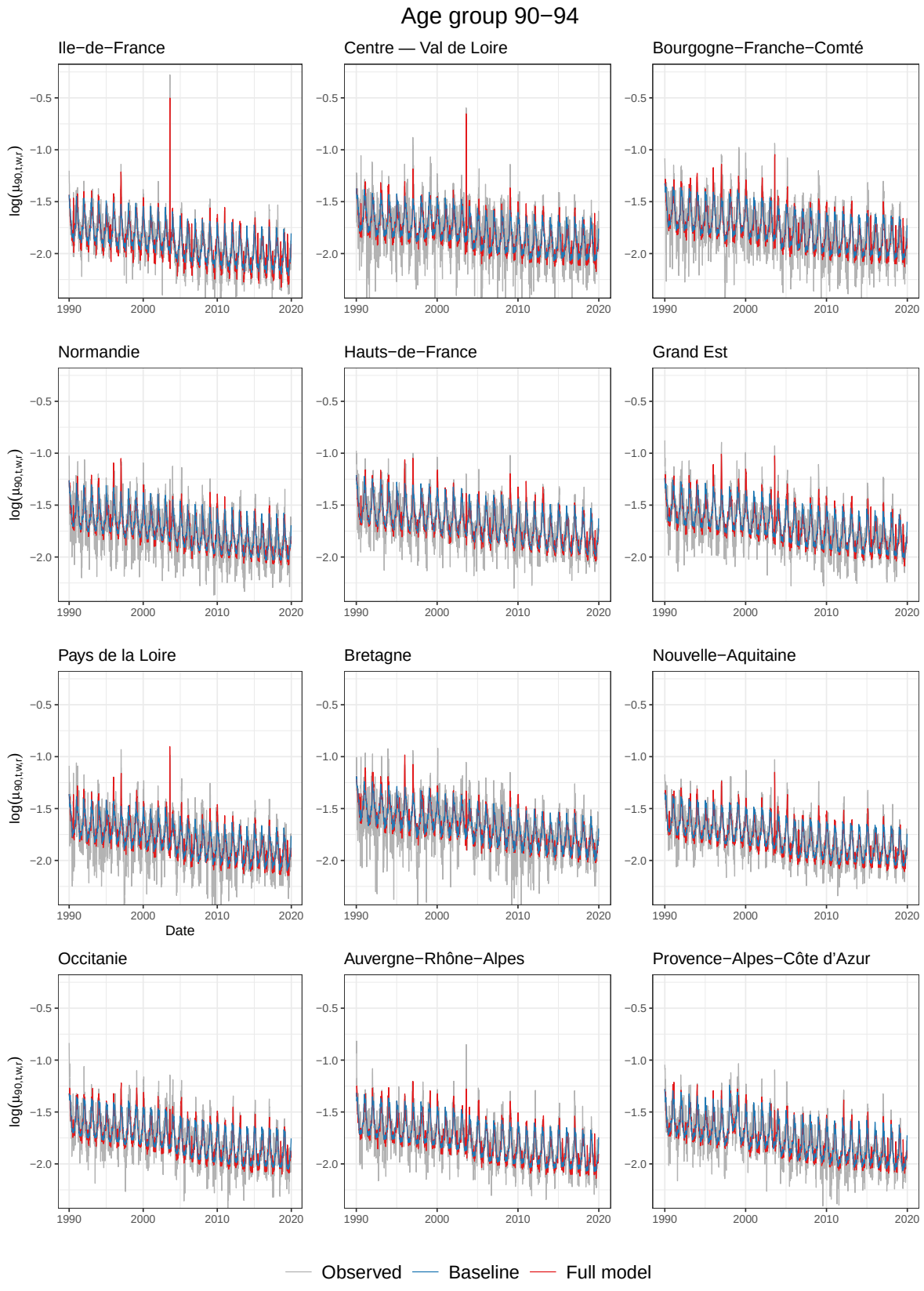

Figure 9: Estimated female weekly death rates from 1990-2019 for the age group 90–94. The gray line represents the logarithm of the observed death rates, while the blue and red line reflect the logarithm of the death rates estimated by the baseline and the full model, including the DLNM component, respectively.

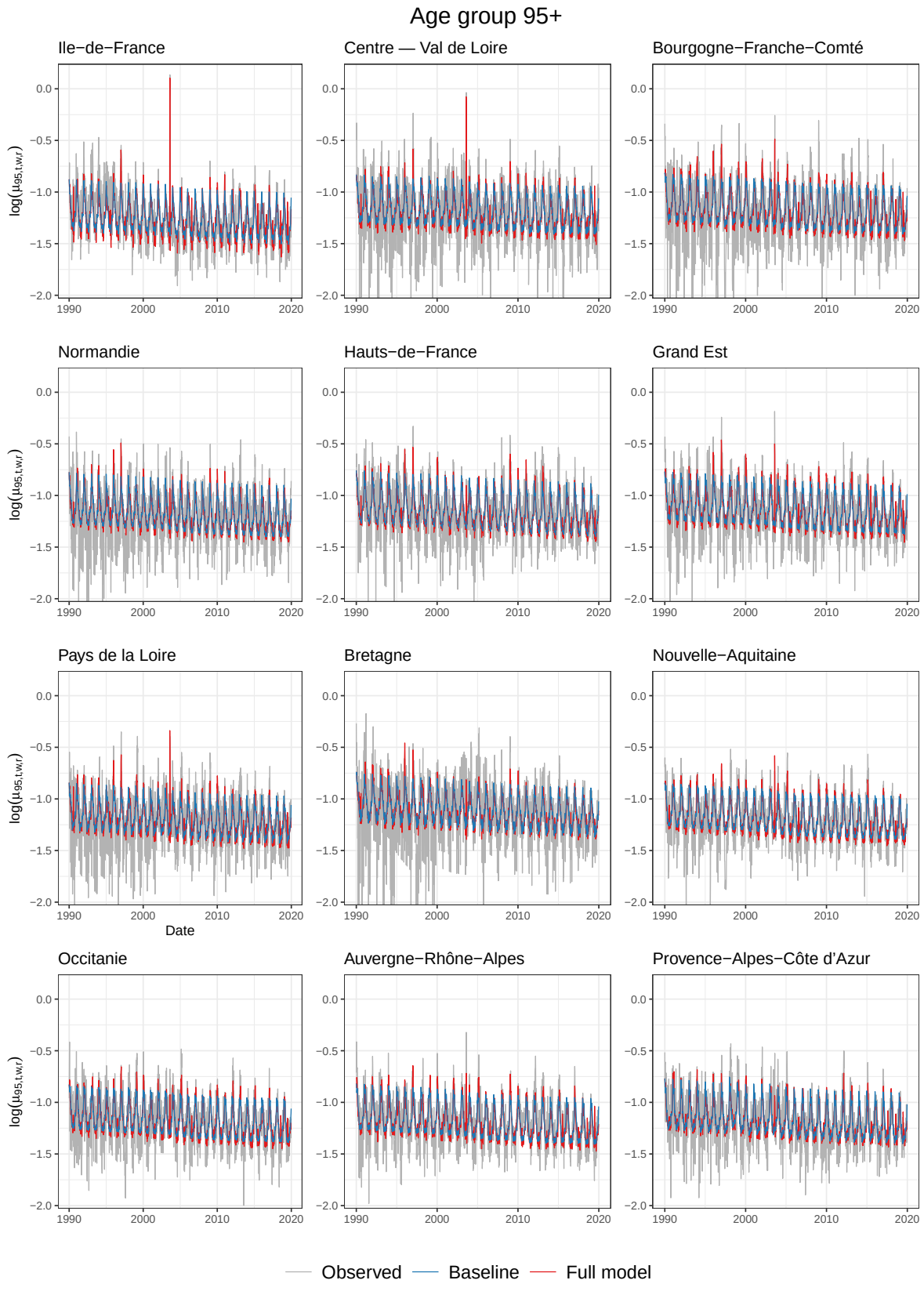

Figure 10: Estimated female weekly death rates from 1990-2019 for the age groups 70-74 (top) and 90-94 (bottom) in Hauts-de-France (left), Bretagne (middle), and Auvergne-Rhône-Alpes (right). The gray line represents the logarithm of the observed death rates, while the blue and red line reflect the logarithm of the death rates estimated by the baseline and the full model, including the DLNM component, respectively.

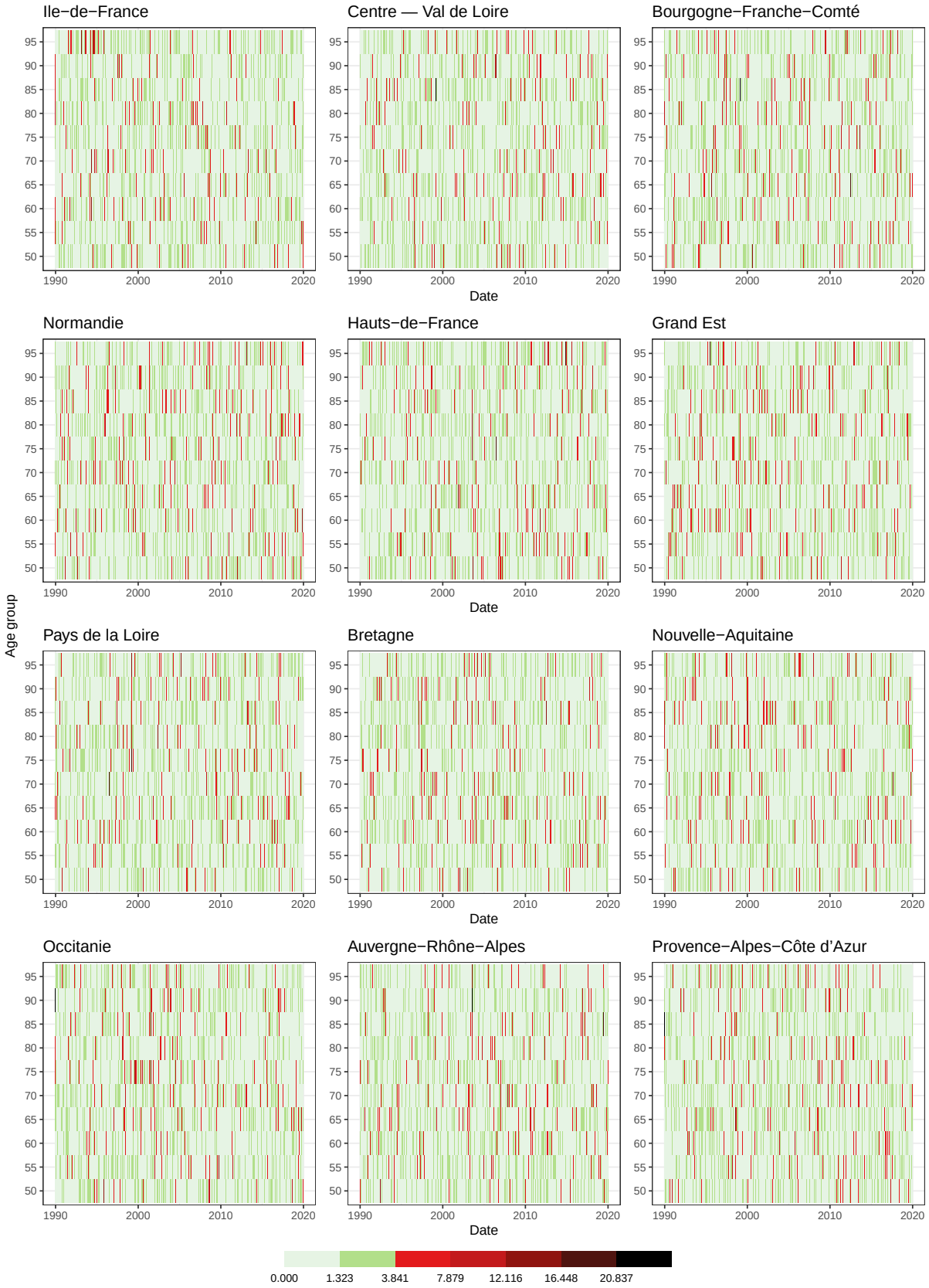

Figure 11: Heat map of the squared Pearson residuals $\rho^2_{x,t,w,r}$ across age and time for the twelve administrative regions in France. Green cells indicate areas with a good fit, while red and black cells correspond to areas with a poor fit ($\rho^2_{x,t,w,r} > \chi^2_1 = 3.841$).

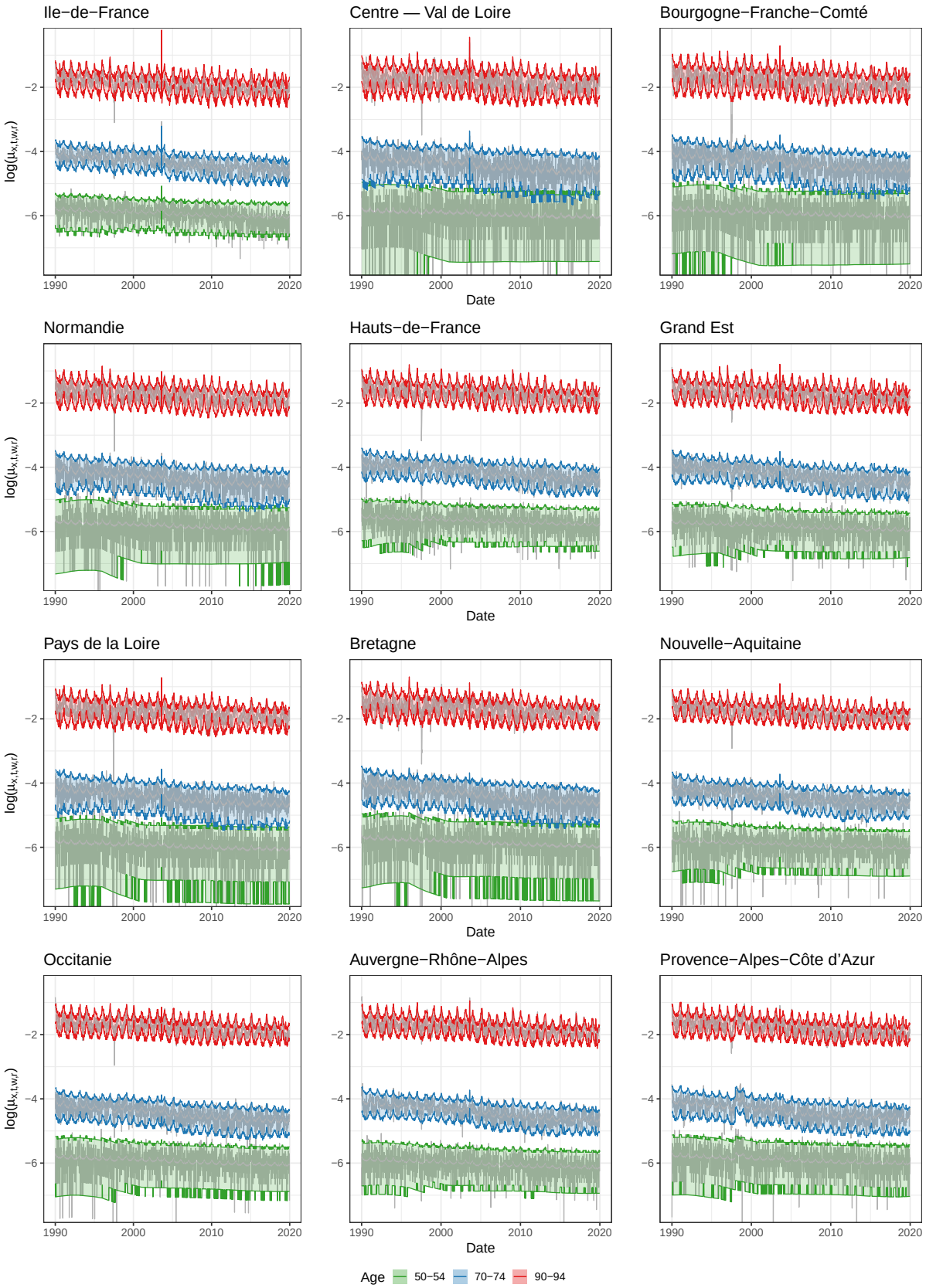

Figure 12: 95% uncertainty bounds around the logarithm of the estimated weekly death rates from 1990-2019 for the age groups 50-54, 70-74 and 90-94 in the twelve administrative regions of France.

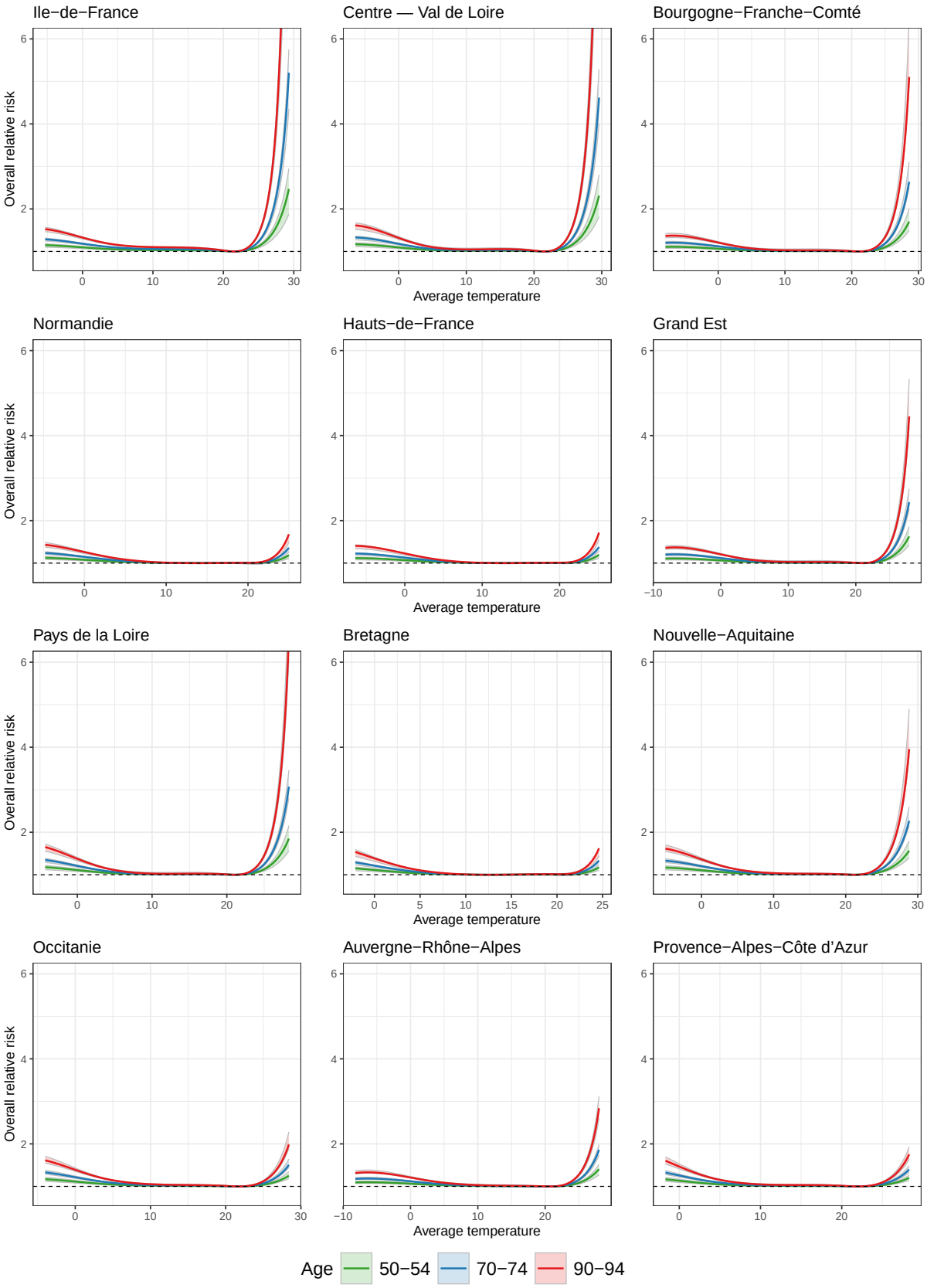

Figure 13: Estimated overall relative risk for temperature in the twelve administrative regions of France for the age groups 50–54, 70–74, and 90–94. Shaded areas represent 95% point-wise confidence intervals.

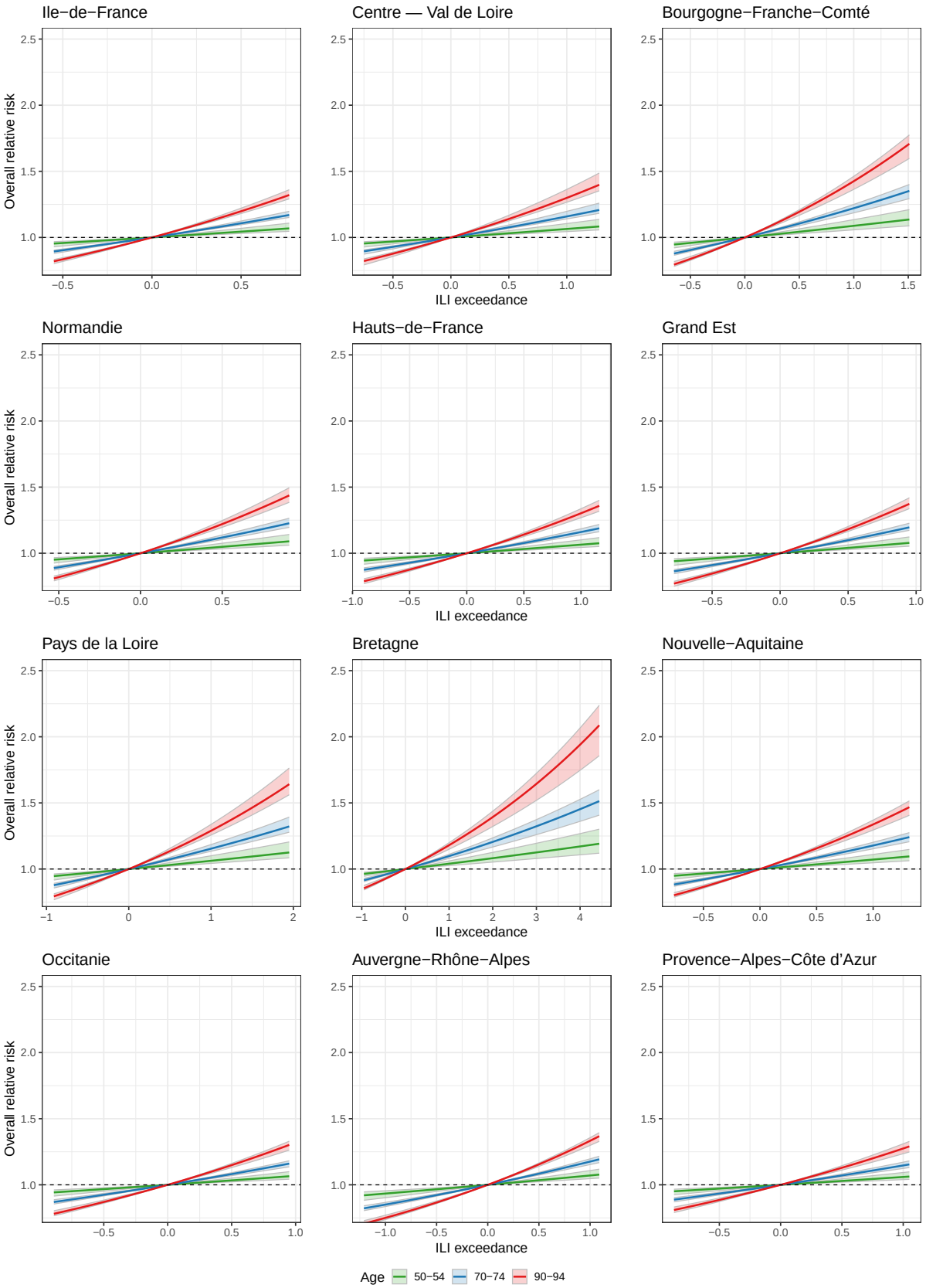

Figure 14: Estimated overall relative risk for ILI exceedance rates in the twelve administrative regions of France for the age groups 50–54, 70–74, and 90–94. Shaded areas represent 95% pointwise confidence intervals.

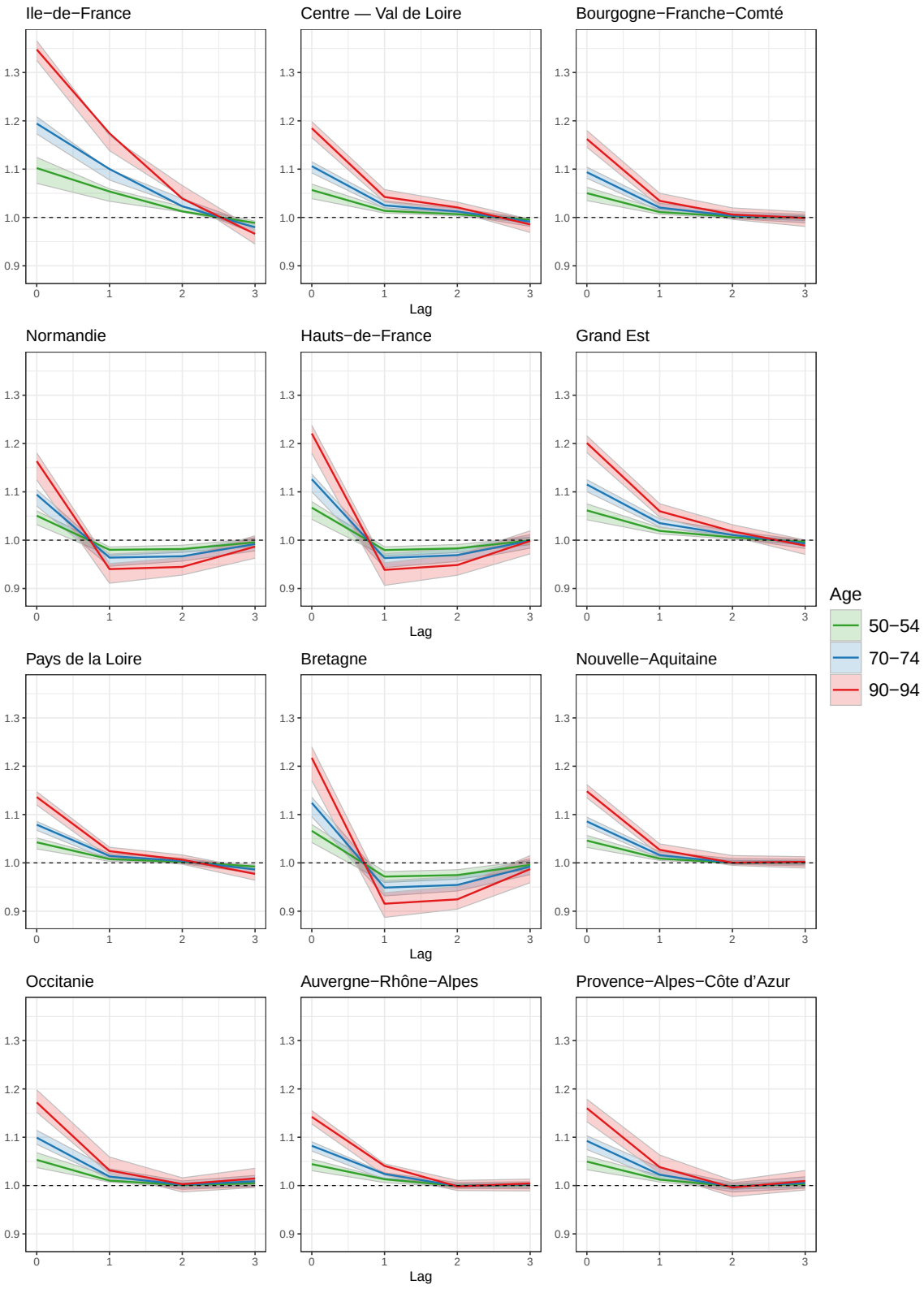

Figure 15: Estimated relative risk per lag at the 99.5th percentile of the region-specific weekly average temperatures in the twelve administrative regions of France for the age groups 50–54, 70–74, and 90–94. Shaded areas represent 95% point-wise confidence intervals.

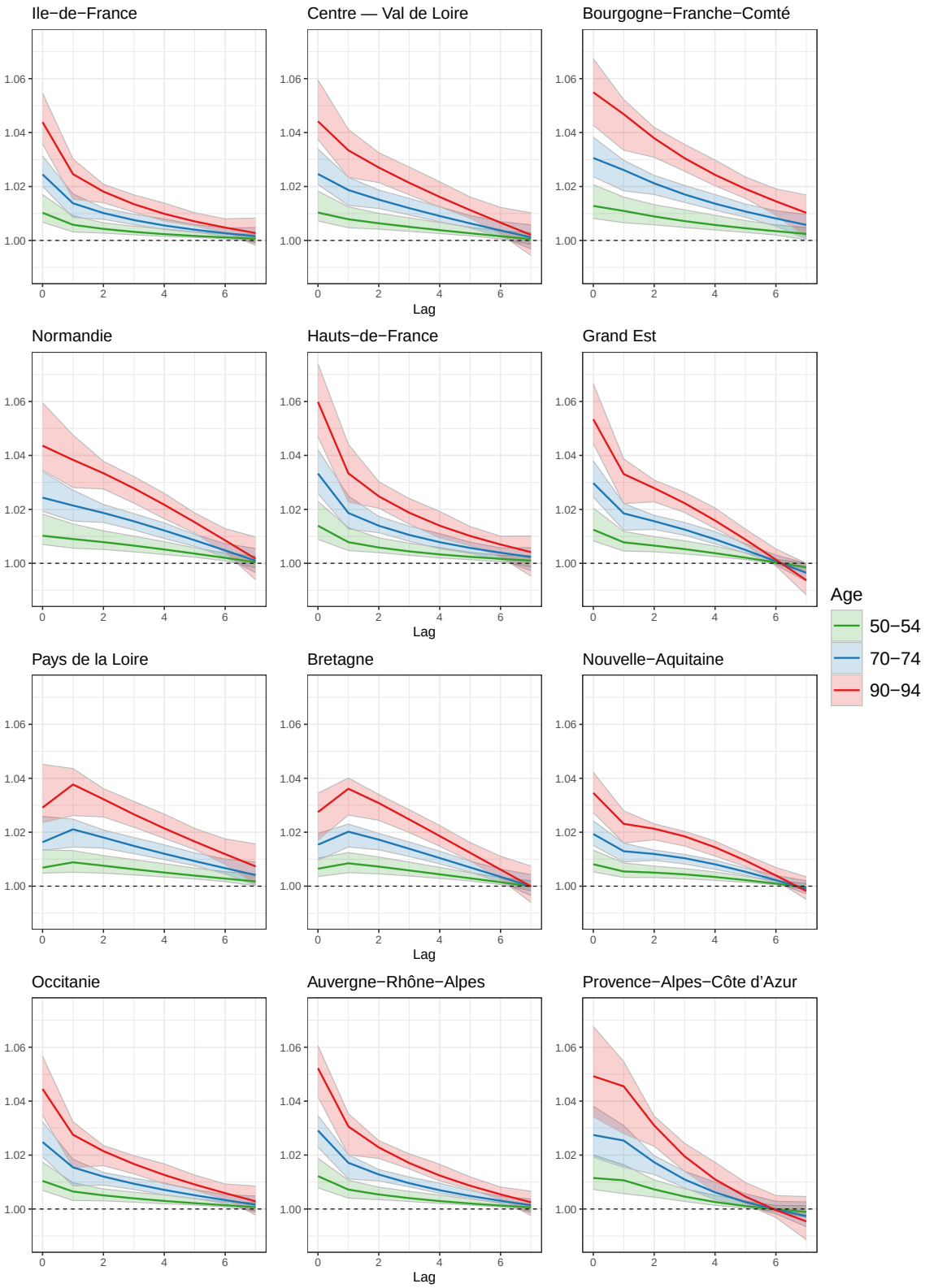

Figure 16: Estimated relative risk per lag at the 99.5th percentile of the region-specific weekly average ILI exceedance rates in the twelve administrative regions of France for the age groups 50–54, 70–74, and 90–94. Shaded areas represent 95% point-wise confidence intervals.

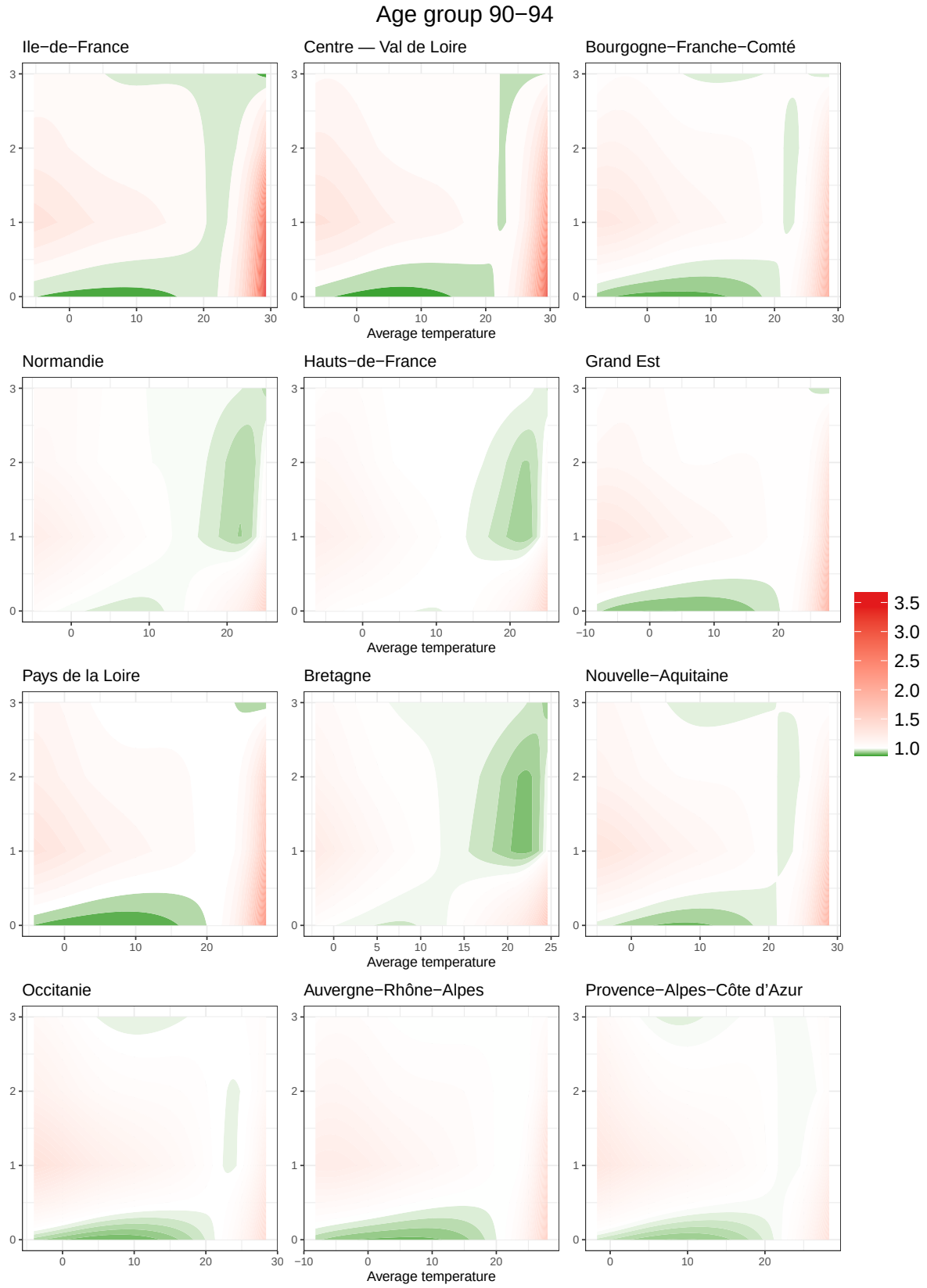

Figure 17: Estimated relative risk (RR) surfaces of the lag-specific temperature–mortality associations in the twelve administrative regions of France for the age group 90–94. Red areas indicate an increased RR, while green areas indicate a decreased RR.

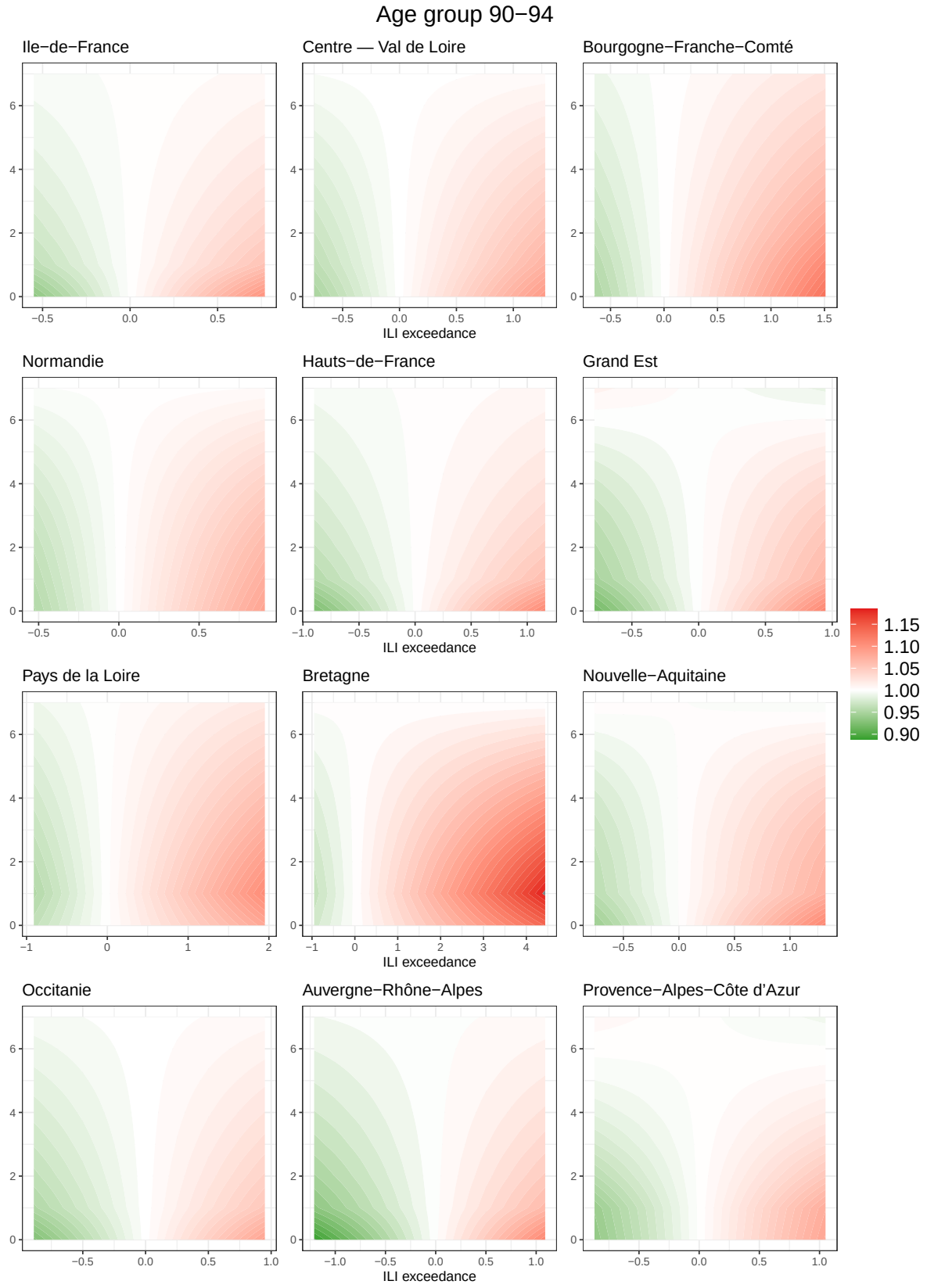

Figure 18: Estimated relative risk (RR) surfaces of the lag-specific ILI–mortality associations in the twelve administrative regions of France for the age group 90–94. Red areas indicate an increased RR, while green areas indicate a decreased RR.